Available online at www.sciencedirect.com
ScienceDirect
Nuclear Physics B Proceedings Supplement 00 (2012) 1–6
Nuclear Physics B Proceedings Supplement

Observation of a New Resonance at ATLAS

Antonio Boveia, on behalf of the ATLAS Collaboration
Enrico Fermi Institute, University of Chicago, 5640 S Ellis Ave, Chicago, IL 60637

Abstract

With the LHC increasing collision energies to $\sqrt{s} = 8$ TeV and delivering luminosity more rapidly than ever, searches for Higgs-like particles at the ATLAS experiment have reached the sensitivities required to detect the Standard Model Higgs boson across a broad range of possible masses. I discuss signals found in searches for Higgs boson decays to both two photons and to ZZ^* to four leptons, announced earlier in July, and present a new search for Higgs boson decays to WW^* with the 2012 data.

Keywords:

1. Introduction

The Higgs mechanism breaks the electroweak symmetry of the Standard Model (SM) and gives mass to its massive fundamental particles through their couplings to the scalar Higgs field. The boson corresponding to this field, the best direct evidence that the mechanism is correct, has been anticipated by generations of particle physics experiments. Though the production cross sections and decay branching fractions of the Higgs boson are, for a given mass m_H, completely determined by well-measured SM parameters, the mass itself is a free parameter that could be anything from tens to hundreds of GeV. The most sensitive searches for the Higgs boson prior to the LHC [1] had collision energies and luminosities large enough to test and exclude some but not all of the possibilities. When combined with fits of the SM to precision electroweak observables, these results point to a mass between 114.4 and 160 GeV [2].

The LHC and its experiments, ATLAS [3] and CMS, are designed to find and study the SM Higgs boson no matter what its mass may be. At the end of 2011, with up to 4.7 fb^{-1} of 7 TeV collision data and a broad assortment of SM measurements completed, ATLAS searches for the Higgs boson in the five most-favored decay modes were able, taken together, to exclude almost all of the possible masses [4]. Of those masses favored by prior experiments, only the ranges (116.6–119.4) GeV and (122.1–129.2) GeV remained viable. The second range, which should have been at least partially excluded, remained because both the $\gamma\gamma$ and $ZZ \to \ell\ell\ell\ell$ searches found slight excesses in the data around 125 GeV. Consequently, this region was set to receive immediate and intense scrutiny when the LHC resumed collisions at $\sqrt{s} = 8$ TeV in 2012.

For 120 GeV $< m_H <$ 130 GeV, a wide variety of decay channels are immediately relevant, but three are of particular interest: $H \to \gamma\gamma$, $H \to ZZ^* \to \ell\ell\ell\ell$, and $H \to WW^* \to \ell\nu\ell\nu$. These are the three most sensitive channels and are the first three ATLAS searches to incorporate the 8 TeV data, up to 5.9 fb^{-1} as of the end of June 2012. Each of these searches refined its methods to increase the sensitivity to a $m_H \approx 125$ GeV Higgs boson. This was done in a blind fashion, using simulation and control data, before examining the data in the region defined by the 2011 excess.

2. $H \to \gamma\gamma$

In the SM, proton-proton collisions do not produce photon pairs through any resonance other than the Higgs boson. Thus the background to the search has a smooth and falling diphoton invariant mass distribution. The signal should appear in this background as a small bump.

The ATLAS search [5, 6] reconstructs the two photons from clusters in the Liquid-Argon electromagnetic calorimeter. Approximately half of all signal events include at least one photon that converts to an electron-positron pair while traversing the material in the inner tracker. These photons are reconstructed by finding the conversion vertices in the tracker.

Much of the background to the search consists of photon-jet or multijet events where one or more photons appears during jet fragmentation. Since these backgrounds are produced with cross sections of up to nine orders of magnitude larger than the signal, powerful photon identification is employed to reduce them. Afterward the dominant backgrounds come from t-channel quark-antiquark annihilation and gluon-gluon interaction with a quark loop, both of which produce two well-isolated photons [7]. An additional, smaller background comes from Drell-Yan events where one or more electrons mimics a photon.

The hadronic and other instrumental backgrounds for single photons are suppressed using finely-segmented measurements of the electromagnetic shower and measurements of calorimeter activity nearby the photon (isolation). The shower measurements include the ability to resolve the two photons from π^0 decay and to extrapolate the origin of the photon longitudinally along the interaction region. The isolation energy is computed within a cone in $\eta - \phi$ of radius 0.4 using clustered energy deposits instead of individual calorimeter cells, in order to reduce residual, well-modeled effects of out-of-time pile-up, and is corrected event-by-event for the ambient energy density due to total pile-up and underlying event activity.

The combined effect of the shower shape and isolation requirements is to reduce the rate at which fragmentation photons are accepted by $\approx 10^4$. The total efficiency of the selection for isolated photons is 85–95%, as measured and checked in samples of $Z\gamma$, $Z \to ee$, and sideband data samples. The efficiencies of both the calorimeter and conversion reconstruction remain stable over the entire range of pile-up conditions found in the data.

The diphoton mass resolution is determined and refined by studying the calorimeter response to electrons in data and in simulation, then extrapolating from electrons to photons using the simulation and studies of material effects. Using samples of $J/\Psi \to ee$, $W \to e\nu$, and $Z \to ee$ data, the electron energy scale has been determined to 0.3% at the Z boson mass, with a linearity of better than 1% and a constant term that is about 1% in the barrel calorimeter and up to 2.5% elsewhere. The corresponding photon energy response has been checked in data with photon conversions, E/p measurements, and other data samples. The energy response in data is stable over time, and the simulated diphoton mass resolution is insensitive to the rapidly-increasing amounts of pile-up observed in the data.

The latest ATLAS result consists of a refined analysis of the 4.8 fb^{-1} recorded at 7 TeV and a search of 5.9 fb^{-1} of 8 TeV data. Each requires one photon with tranverse momentum $p_T > 40$ GeV and isolation energy less than 4 GeV, and another isolated photon with $p_T > 30$ GeV, then divides the data sample into populations with similar sensitivity and compares the observed diphoton mass distribution in the data to a data-driven background prediction.

Because simulation-based estimates of the background are subject to theory uncertainties that are large relative to the expected signal, and to potential mismodeling of the large rejection factors obtained by selecting only the rare tails of jet fragmentation distributions, the backgrounds are estimated by fitting the mass distribution in the data. Candidate events are divided into ten categories: nine categories defined by the diphoton topology, the pseudorapidities of the photons, and whether or not the photons have converted; and a new, tenth category for for events produced via vector boson fusion (VBF) with ≥ 2 accompanying forward jets. The diphoton mass distribution of the data in a given category is fit separately to obtain the background prediction for that category.

The choice of the background functions is critical. Each function must have the flexibility to match the shape of the background in the data, so as to avoid spurious signals, but it must not be so flexible that it would obscure a potential signal. A large menu of possible functions was considered for each category, including single and double exponentials, polynomials of various orders, and exponentials of polynomials. Each function was validated against a high-statistics simulation of all backgrounds and against sideband data. For each event category, the function with the best expected sensitivity was chosen from all functions giving potential biases of less than 10% of the expected signal or less than 20% of the expected uncertainty on the fitted signal yield. The spurious signal obtained fitting the chosen function plus a signal parameterization to the background-only simulation was then assigned as a systematic uncertainty due to the choice of the function.

Figure 1 shows the diphoton mass distribution for the data and background fits summed over all ten categories and the two datasets. The maximum deviation from the

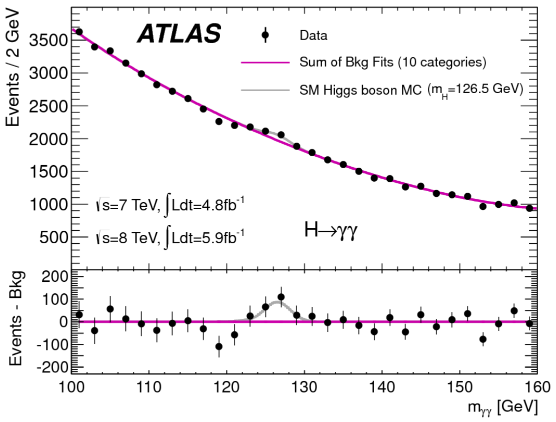

Figure 1: The diphoton mass distribution for the combined 7 TeV and 8 TeV datasets [6]. The heavier line indicates the sum of the background fits over all ten categories and the two datasets. The lighter line indicates the expectation for a $m_H = 126.5$ GeV signal.

background expectation occurs at $m_H = 126.5$ GeV with a local significance of 4.5σ, with 2.4σ expected on average for a Higgs boson produced at the nominal SM rate. The global significance, correcting for the look-elsewhere effect between (110–150) GeV, is 3.6σ. The excess is evenly split between the 7 and 8 TeV datasets. A similar analysis performed without categories on the combined data, using a single 4th-order polynomial background function, finds 3.5σ significance before a small $(0.1\text{–}0.2)\sigma$ correction for the photon energy systematic uncertainty. The best-fit signal strength across the ten categories for $m_H = 126.5$ GeV is 1.9 ± 0.5 times the SM prediction. The signal strengths found individually for each category are compatible with the combined strength.

3. $H \to ZZ^* \to \ell\ell\ell\ell$

The search for $H \to ZZ^*$ to four leptons [6, 8] is clean and simple: select four isolated electrons or muons and look for a peak in the four-body invariant mass. The requirement of four leptons already reduces most backgrounds to a negligible level, and the remaining backgrounds are small.

A many-lepton signal requires high reconstruction and identification efficiencies across a large detector acceptance. With assumed Higgs boson masses well below $2m_Z$, one or more of the leptons is often forward or very low p_T, and the signal yield depends on lepton efficiencies to the fourth power. The small backgrounds to the search allow relaxed, high efficiency electron and muon identification requirements, with isolation and impact parameter selections rejecting most of the hadronic backgrounds. The resulting four-lepton efficiency is 17–23% (for $4e$) up to 41–43% (for 4μ).

The search selects events containing four leptons with $p_T \geq 20, 15, 10, 7/6$ GeV, where the minimum allowed p_T for the lowest p_T lepton is 1 GeV lower when that lepton is a muon, then requires a opposite-sign same-flavor lepton pair with dilepton mass 50 GeV $< m_{12} <$ 106 GeV and another pair with a minimum mass requirement that varies from 17.5 GeV for $m_{4\ell} = 120$ GeV to 22.5 GeV for $m_{4\ell} = 130$ GeV. The value of m_{12} is then constrained to m_Z. The four-body mass resolution is then between 1.8 GeV (4μ) to 2.5 GeV ($4e$).

The dominant background to the search is continuum ZZ, the leading source of four-real-lepton events in the SM. This is taken from simulation. The other backgrounds are a mixture of Z + jets and top events, where one or more of the lepton candidates are mis-identified hadronic backgrounds. For Z + jets events where the jets mimic a low-mass muon pair, the hadronic background model consists of $t\bar{t}$ and $Z + bb$ contributions derived from bb-enriched control data, where the low-mass dimuon pair fails the impact parameter requirement and the isolation requirement is removed. For Z + jets where the jets mimic a low-mass electron pair, the backgrounds from photon conversion, hadronic fakes, and semileptonic heavy-flavor decays are derived from sidebands in several electron identication variables that discriminate between the three components (such as the presence of a hit in the innermost tracking layer).

Fig. 2 shows the four-lepton mass distributions observed in the 7 TeV and 8 TeV data and the background models. For $m_{4\ell} > 160$ GeV, where continuum ZZ dominates and no signal is expected, the data contain a broad excess of 20–30% more events than predicted. These events are consistent with ZZ production and the overall increase in the rate is similar to the one observed in prior ATLAS measurements of the ZZ cross section [9, 10]. Therefore the ZZ background prediction for the search is renormalized to the observed rate.

For 120 GeV $< m_{4\ell} <$ 130 GeV, 5.1 ± 0.3 background events are predicted and 13 events are observed. The distribution of this excess across channels is consistent with ZZ decay and is divided properly between the 7 and 8 TeV datatsets . The largest deviation from the background occurs for $m_H = 125$ GeV, with 3.4σ local significance. The excess is compatible with the 5.3 ± 0.4 events expected for the SM Higgs boson. The best-fit signal strength is 1.3 ± 0.6 times the SM prediction.

4. $H \to WW^* \to \ell\nu\ell\nu$

The two-lepton two-neutrino final state is neither simple nor clean. The large $H \to WW^*$ branching fraction (23% at m_H = 125 GeV) results in a large signal yield, but due to the two unreconstructed neutrinos it appears as a broad excess in tranverse mass. The backgrounds are a complex mixture of continuum WW[11], WZ/ZZ [12], $W\gamma/\gamma^*$ [13], W + jets [14], Drell-Yan [15], and top [16] events. Reconstructing the signal and reducing the backgrounds involves all of the detector. Because it lacks a peaking signal, it is largely a counting experiment in which all of these elements need to be understood to a challenging level of precision.

The analysis selection is discussed in detail in Ref. [6] and [17]. Starting with exactly two opposite-charge electrons or muons with $p_T > 25, 15$ GeV, events are selected with high missing transverse momentum, low dilepton mass, high dilepton p_T, and a small azimuthal angle between the leptons. This exploits differences between the signal, the spin-0 decay, and the Drell-Yan, $W + \gamma/\gamma^*$/jets, and WW backgrounds. The 7 TeV analysis was done separately for ee, $e\mu$, and $\mu\mu$ events to take advantage of the lower Drell-Yan background to $e\mu$ events. The 8 TeV analysis was performed only for $e\mu$ events due to the increased difficulty of dealing with the Drell-Yan backgrounds in the same-flavor channels with more pile-up. Because the top background increases rapidly as the number of jets allowed in the event increases, the analysis is further divided into three categories with 0, 1, and ≥ 2 jets. As the number of jets increases, additional requirements balancing event transverse momentum and vetoing b tagged jets are applied. The requirements for ≥ 2 jets select the topologies with two forward jets expected when VBF produces a Higgs boson.

The background predictions come from a hybrid of simulation and control data. The WW prediction from simulation is re-normalized to match the yield observed in high-$m_{\ell\ell}$ control data, by a factor of 1.06 ± 0.06 for the 0-jet analysis and 0.99 ± 0.15 for the 1-jet analysis. The $t\bar{t}$ and single top prediction is re-normalized to control data where one or more of the jets accompanying the leptons has been b-tagged. The 1-jet factor is 1.11 ± 0.05 and the ≥ 2-jet factor is 1.05 ± 0.01. The normalization for 0-jet events, which lack a jet to b-tag, is obtained by correcting the jet veto efficiency in simulation using the fraction of events with zero additional jets found in a sample of events with at least one b-tag. The total 0-jet factor is 1.11 ± 0.06.

The background from W + jets events is estimated by measuring the rate for jets to be mis-identifed as leptons in the data and applying this in situ to events with anti-identified leptons in the nominal data. This mis-identification rate is measured in samples of dijet events to a precision of about 40%, and the resulting W + jets prediction is checked against control data with same-charge lepton pairs that is otherwise selected as in the nominal analysis. These samples also provide a check of the normalization and shape of the $W\gamma$ and $W\gamma^*$ predictions obtained from simulation.

Fig. 3 shows the transverse mass distribution of the two leptons and the missing transverse momentum obtained by the above procedure for events with 0-jet and 1-jet events in the 8 TeV data. After requiring $0.75 < m_T/m_H < 1$, assuming m_H = 125 GeV, 185 events are observed in the 0-jet data with 142 ± 16 background events predicted. For the 1-jet analysis, 38 events are observed with 26 ± 6 background predicted. For the ≥ 2-jet analysis, no events are observed and 0.35 ± 0.18 background events are predicted. Thus, both 0-jet and 1-jet analysis exhibit excesses.

In all three cases the excesses are compatible with a m_H = 125 GeV signal (20 ± 4, 5 ± 2, and 0.34 ± 0.07 events respectively). The excesses are distributed evenly between events where the leading-p_T lepton is an electron and events, with a different mix of backgrounds, where the leading lepton is a muon. Combining the 8 TeV analysis with the 7 TeV analysis [17], which did not find an excess, and incorporating a fit to the binned m_T distributions, the p-value at m_H = 125 GeV corresponds to 2.8σ and the best-fit signal strength is 1.4 ± 0.5 times the SM expectation.

5. Summary and Outlook

Following this conference, the above results were finalized and published as Ref. [6]. Combined with previous results not discussed here, ATLAS searches exclude a SM Higgs boson with a mass from (111–122) GeV and (131–559) GeV at 95% confidence level. The excess observed in the $\gamma\gamma$, $ZZ^* \to \ell\ell\ell\ell$ and $WW^* \to \ell\nu\ell\nu$ searches corresponds in the combined search to a maximum local significance, 5.9σ, for a Higgs boson mass of m_H = 126.5 GeV. The excess is consistent with the SM Higgs boson hypothesis across multiple decay channels, within subchannels of the individual searches, and between 7 and 8 TeV datasets. Fig. 4 shows the individual and combined best-fit signal strength μ for the five most-favored decay modes. Fig. 5 shows confidence intervals in the μ–m_H plane for the three channels discussed here.

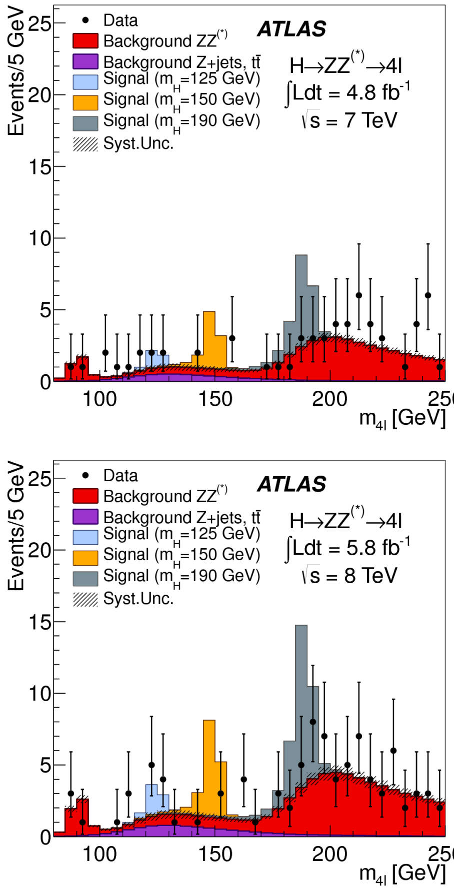

Figure 2: The four-lepton mass distribution for the 7 TeV and 8 TeV datasets [6].

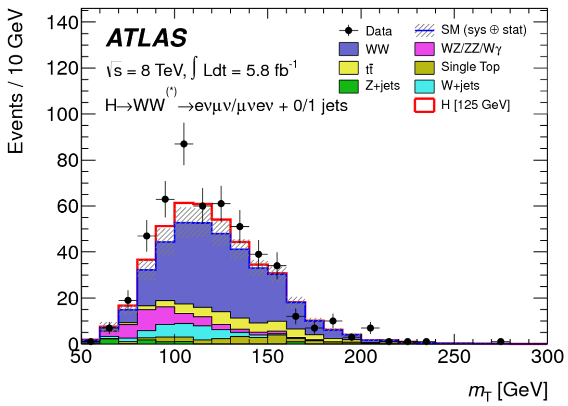

Figure 3: The transverse mass distribution of leptons and missing transverse momentum in events selected by the 0-jet and 1-jet analyses of 8 TeV data in the $e\mu$ and μe channels [6]. The hashed area indicates the total uncertainty on the background prediction. The expectation for a 125 GeV signal is stacked on top of the backgrounds.

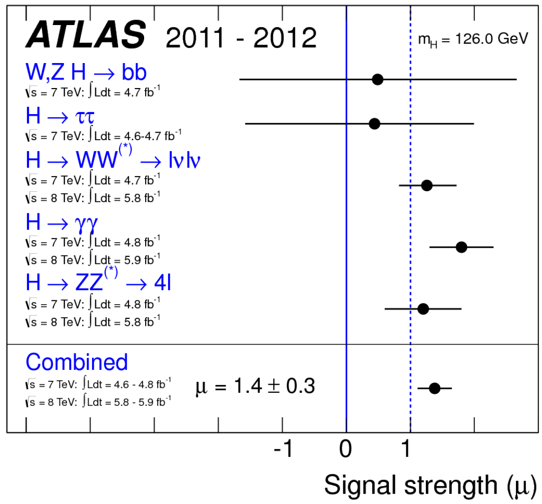

Figure 4: Measurements of the signal strength parameter μ for m_H = 126 GeV for the individual channels and their combination [6].

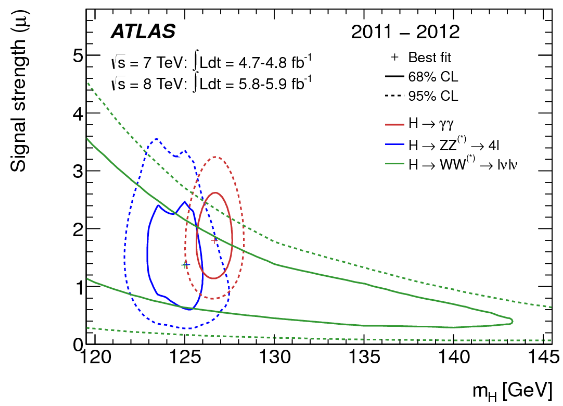

Figure 5: Confidence intervals in the $\mu - m_H$ plane for the $\gamma\gamma$, $ZZ^* \rightarrow \ell\ell\ell\ell$, and $WW^* \rightarrow \ell\nu\ell\nu$ searches including all systematic uncertainties [6]. The markers indicate the maximum likelihood estimates for each search.

References

[1] Precision Electroweak Measurements and Constraints on the Standard Model, arXiv:1012.2367.

[2] M. Baak, M. Goebel, J. Haller, A. Hoecker, D. Ludwig, et al., Updated Status of the Global Electroweak Fit and Constraints on New Physics, Eur. Phys. J. C72 (2012) 2003.

[3] ATLAS Collaboration, The ATLAS Experiment at the CERN Large Hadron Collider, JINST 3 (2008) S08003.

[4] ATLAS Collaboration, Combined search for the Standard Model Higgs boson in pp collisions at $\sqrt{s}$ = 7 TeV with the ATLAS detector, Phys. Rev. D86 (2012) 032003..

[5] ATLAS Collaboration, Search for the Standard Model Higgs boson in the diphoton decay channel with 4.9 fb^{-1} of pp collisions at $\sqrt{s}$ = 7 TeV with ATLAS, Phys. Rev. Lett. 108 (2012) 111803.

[6] ATLAS Collaboration, Observation of a new particle in the search for the Standard Model Higgs boson with the ATLAS detector at the LHC, Phys. Lett. B716 (2012) 1–29.

[7] ATLAS Collaboration, Measurement of the isolated di-photon cross-section in pp collisions at $\sqrt{s}$ = 7 TeV with the ATLAS detector, Phys. Rev. D85 (2012) 012003.

[8] ATLAS Collaboration, Search for the Standard Model Higgs boson in the decay channel $H \to ZZ^* \to 4\ell$ with 4.8 fb^{-1} of pp collision data at $\sqrt{s}$ = 7 TeV with ATLAS, Phys. Lett. B710 (2012) 383–402.

[9] ATLAS Collaboration, Measurement of the ZZ production cross section and limits on anomalous neutral triple gauge couplings in proton-proton collisions at $\sqrt{s}$ = 7 TeV with the ATLAS detector, Phys. Rev. Lett. 108 (2012) 041804.

[10] ATLAS Collaboration, Measurement of the total ZZ production cross section in the four-lepton channel using 5.8 fb^{1} of ATLAS data at $\sqrt{s}$ = 8 TeV, Tech. Rep. ATLAS-CONF-2012-090, CERN, Geneva (Jul 2012).

[11] ATLAS Collaboration, Measurement of the WW cross section in $\sqrt{s}$ = 7 TeV pp collisions with the ATLAS detector and limits on anomalous gauge couplings, Phys. Lett. B712 (2012) 289–308.

[12] ATLAS Collaboration, Measurement of the WZ production cross section and limits on anomalous triple gauge couplings in proton-proton collisions at $\sqrt{s}$ = 7 TeV with the ATLAS detector, Phys. Lett. B709 (2012) 341–357.

[13] ATLAS Collaboration, Measurement of $W\gamma$ and $Z\gamma$ production in proton-proton collisions at sqrt(s)=7 TeV with the ATLAS Detector, JHEP 1109 (2011) 072.

[14] ATLAS Collaboration, Study of jets produced in association with a W boson in pp collisions at $\sqrt{s}$ = 7 TeV with the ATLAS detector, Phys. Rev. D85 (2012) 092002.

[15] ATLAS Collaboration, Measurement of the production cross section for Z/γ^* in association with jets in pp collisions at $\sqrt{s}$ = 7 TeV with the ATLAS detector, Phys. Rev. D85 (2012) 032009.

[16] ATLAS Collaboration, Measurement of the cross section for top-quark pair production in pp collisions at $\sqrt{s}$ = 7 TeV with the ATLAS detector using final states with two high-p_T leptons, JHEP 1205 (2012) 059.

[17] ATLAS Collaboration, Search for the Standard Model Higgs boson in the $H \to WW^* \to \ell\nu\ell\nu$ decay mode with 4.7 fb^{-1} of ATLAS data at $\sqrt{s}$ = 7 TeV, Phys. Lett. B716 (2012) 62–81.